Preprint
UCRL-JC-137904

10 μm and 5 μm Pinhole-Assisted Point-Projection Backlit Imaging for NIF

A. B. Bullock, O. L. Landen, D. K. Bradley

This article was submitted to
The Thirteenth Topical Conference on High-Temperature Plasma Diagnostics, Tucson, AZ
June 18-22, 2000

June 5, 2000

U.S. Department of Energy

Lawrence
Livermore
National
Laboratory

10 μm and 5 μm Pinhole-Assisted Point-Projection Backlit Imaging for NIF, A. B. Bullock, O.L.Landen, and D.K. Bradley, *Lawrence Livermore National Laboratory, Livermore CA.*

Pinhole-assisted point-projection backlighting with 10 μm and 5 μm pinholes placed a small distance of order 1mm away from the backlighter produces images with large field of view and high resolution. Pinholes placed closely to high-power backlighter sources can vaporize and close due to x-ray driven ablation, thereby limiting the usefulness of this method. A study of streaked 1-D backlit imaging of 25 μm W wires using the OMEGA laser is presented. The pinhole closure timescale for 10um pinholes placed 0.45 mm and 1 mm distant from the backlighter is 1.3 ns and 2.2 ns, respectively. Similar timescales for 5 um pinholes is also presented. Successful wire imaging prior to pinhole closure is clearly demonstrated.

Introduction

Radiographic imaging of high-density samples using x-ray backlighting is an important diagnostic technique in high energy density experiments such as those performed on NOVA[1] and OMEGA[2] laser facilities. Experiments involving both laser-driven ablation[3,4,5] and x-ray driven ablation have used x-ray backlighting to probe physical details in high samples too opaque to allow optical probing. Many of these experiments use laser-driven foils to produce the imaging x-rays, and these x-rays image

the experimental sample in two typical geometries. In the area-backlighter geometry (see figure 1(A)), the laser interacts with the foil backlighter to produce a plasma, and this plasma illuminates the sample. An imaging pinhole is placed behind the sample to image the shadow on to a static or framing x-ray camera. Use of the pinhole provides well-characterized image resolution, and the large backlighter plasma size helps produce a long-lived x-ray source by mitigating the effect of energy loss at the plasma edges. However, the area-backlighter geometry requires a backlighter plasma to be equal to or greater than the sample in size, and this generates unreasonably large backlighter power requirements for larger future facilities such as NIF[6].A second geometry (see figure 1(B)), the point projection geometry, uses a small target such as a fiber or foil to produce an x-ray point source, and this x-ray source produces a shadow of the sample which is projected on to the camera. This method avoids the NIF-related size limitation, but due to greater plasma cooling due to edge energy losses, the point source is a less efficient radiator. In addition, the resolution is degraded after a few 100 ps due to plasma expansion speeeds of 100-300 μm/ns.

A third geometry, pinhole-assisted point-projection backlighting (see figure 1 (C)), offers a useful alternative. A large backlighter plasma is produced as a source, and a pinhole is placed between the source and the sample. In this way, the pinhole acts much like a point source illuminating the sample on to the camera. This method can image large targets without requiring a large plasma size, and this x-ray source is long-lived.

However, imaging of large-sized samples requires the pinhole to be placed small distances (of order 1mm) away from the backlighter. Pinholes placed this distance from the backlighter can receive incident x-ray intensities of order 1 GW/cm^2 at the pinhole walls, and these intensities are sufficient to drive ablation. In the case of high-resolution imaging using small (~<10 μm) pinholes, this ablation can cause the pinhole to fill with ablated material, thereby causing the x-rays transmitted through the pinhole to be absorbed and effectively 'closing' the pinhole.

Using 10 μm and 5 μm pinholes, we studied the effect of pinhole closure on pinhole-assisted point-projection imaging using a 4.7 keV Ti backlighter. Streak camera images of W wires produced by these pinholes are analyzed to infer time-dependent pinhole transmission and pinhole size. The pinhole transmission results are compared to a simple model of pinhole transmission. This model is based on x-ray driven Ta wall ablation, which is assumed to occur after the Ta wall temperature has exceeded the Ta boiling temperature. The measured pinhole transmission agrees with calculated results.

Experimental Description

Ablation and closure of 5 μm and 10 μm pinholes during point-projection backlit imaging was studied with the method described below. The targets consisted of a 12.7 μm Ti backlighter foil, a 'primary' pinhole, 10 μm or 5 μm in diameter, and a 'reference' pinhole, 23 μm in diameter, (see figure 2). The 'primary ' pinhole is positioned at a

distance at which pinhole ablation and closure are expected in the 2 ns timescale. The larger 'reference' pinhole is positioned a greater distance from the backlighter and is not expected to close. This allows the monitoring of backlighter intensity by monitoring x-ray emission through this 'reference' pinhole. The backlighter foil is placed on edge on a 100 μm polycarbonate base. The 'primary' pinhole is composed of a 50 μm Ta substrate with a laser-cut hole (either 10.5 ± 0.5 μm or 5 ± 0.5 μm in diameter) in the center of the substrate. This pinhole is placed on the base a small distance (either 0.45 mm or 1mm) from the backlighter foil. The 'reference' pinhole pinhole is also composed of a 50 μm Ta substrate with a laser-cut hole (23 ± 2 μm in diameter) in the center of the substrate. This pinhole is placed 1.5 mm away from the backlighter foil. A set of three 25 μm W wires is placed 1.5 mm away from both the'primary' and 'reference' pinhole. Wire-to-wire separation in each set is approximately 100 μm. A x-ray streak camera is placed 15 cm behind each pinhole to record the x-ray emission through the pinhole as a function of time.

During the experiment, the backlighter front surface is illuminated with six 3ns, 351 nm laser pulses from the Omega Laser[7]. The laser spot size at the foil is 250 μm, the total beam energy on target is 1.7 kJ, and the intensity is 10^{15} W/cm^2. The He-like n=2-1 X-rays emitted from the resulting plasma propagate through theTi essentially unattenuated. These x-rays propagate through each pinhole and illuminate the W wire set.

The wires are imaged at 130x magnification onto the photocathode slit of the streak camera, producing a swept (120ps/mm) 1-D image of the W wire shadow. The resulting film image then shows the time history (30 ps resolution) of the 1-D wire shadow produced with the pinhole.

The Ti backlighter and each pinhole function as a point-source of x rays . Streaked images of the wire shadow have a spatial resolution which is dependent both on the resolution of the streak camera itself ($\sigma/M \approx 1$ um) and the finite dimensions of the x-ray pinhole. The latter dependence is shown in the expression[8]

$$\sigma^2 = (\frac{(M+1)}{M} D)^2 + (2.44\lambda \frac{p}{D})^2 \qquad (1),$$

where D is the pinhole diameter, M is the magnification (M≈130 in this experiment), p is the distance from the backlighter to the pinhole, and λ is the characteristic wavelength.

Experimental Results

Figure 3 shows streaked images produced by the 'primary' 10 μm pinhole (A) and the 'reference' 23 μm pinhole (B). Here, the 10 μm pinhole was placed 0.45 mm away from the backlighter. The wire shadow produced with the 10 μm pinhole is clearly visible after 500 ps. Similarly, the wire shadow produced by the 23 μm pinhole is visible at 2ns, which implies that the 23 um pinhole does not ablate and close appreciably on this

timescale. The time-dependent intensity of the x-rays propagating through the 10 μm pinhole is measured from the streaked image in the region adjacent to the wire shadow. The time-dependent intensity of the x-rays propagating through the 23 μm pinhole is also measured, and this intensity is assumed to correspond to the relative backlighter source intensity. By normalizing the x-ray intensity from the 10 μm pinhole to the relative backlighter intensity, a plot of 10 μm pinhole transmission is produced (see figure 4). The plot shows that the pinhole transmission value is approximately unity until 500ps after start of the backlighter. At that point, the transmission drops sharply. This delay suggests that there is a threshold Ta surface temperature which must be exceeded before appreciable ablation can occur. The plot also shows the pinhole timescale to be approximately 1.3 ns. Point-projection backlit imaging using 10 μm pinholes 0.45mm away from the backlighter is therefore limited to times less than 1.3 ns. The timescale for the pinhole transmission to drop to 50% is 0.8 ns. Figure 4 also shows transmission for a 10 μm pinhole pinhole placed 1mm away from the backlighter. In this case, transmission stays constant until approximately 900 ps after start of the backlighter, suggesting that the temperature of the pinhole wall surface increases more slowly than the '0.45 mm distance' case. The pinhole closure time is also longer, and by interpolating from the plot, the timescale is estimated to be 2.2 ns. The timescale for the pinhole transmission to drop to 50% is 1.5 ns. Similarly, figure 5 shows the time-dependent transmission of a 5 μm

pinhole placed 1mm away from the backlighter. The 5 um pinhole begins to close 200 ps after start of the backlighter, and the timescale for full closure is approximately 600 ps. The timescale for the pinhole transmission to drop to 50% is 0.5 ns.

It is important to understand the ablation dynamics that cause pinhole closure. X-ray driven ablation of the pinhole wall causes Ta to expand into the pinhole. These Ta atoms absorb the x-rays which propagate into the pinhole, and the level of pinhole transmission is therefore dependent on n(r), the Ta atomic density profile inside the pinhole (see figure 6). Since the mean free path of 4.7 keV x-rays in solid density Ta is 1 μm and the pinhole depth , L, is 50 μm, a Ta atomic density of $0.02*n_{solid}$ should be sufficient to drop transmission to 37%. In the case of a steep density profile near $n=0.02*n_{solid}$, the total spatially integrated transmission will be approximately equal to the ratio of $\pi r_1^2/\pi r_0^2$, where r_0 is the radius of the pinhole and r_1 is the radial point at which $n(r_0)= 0.02*n_{solid}$. Thus, a change in transmission value would correspond to a change in effective pinhole radius according the expression $r_1= r_0T^{0.5}$, where T is the transmission, r_1 is the effective radius of the pinhole, and r_0 is the initial radius of the pinhole prior to the experiment. This would be expected to improve image resolution, since image resolution is dependent on pinhole diameter by Eq. (1).

The relationship between pinhole diameter and transmission is studied by measuring the resolution of 1-D W wire shadow images produced by the pinhole. Figure 7 (A) shows a plot of the 1-D wire shadow image 576 ps after the start of the backlighter. This wire shadow image was produced by a 10 μm pinhole placed 0.45mm away from

the backlighter, and the plot was produced by time averaging over the temporal range of 456 to 696 ps. Also shown is a calculated model of the wire shadow. This model is calculated by convoluting an infinitely sharp model of the wire shadow with the point spread function of a 10.6 μm pinhole and the streak camera. We measure the resolution of the experimental wire shadow image by calculating the χ^2 goodness-of-fit between the experimental wire shadow and the modeled wire shadow. The diameter of the pinhole used in calculation of the model is varied until best fit is found. The measured resolution as a function of time is plotted in figure 8.

In the case of a steep, 'hard aperture' density profile, the effective diameter of the pinhole would be transmission-dependent, and a plot of the expected pinhole diameter is also shown in figure 8. Clearly, the measured pinhole diameter does not agree with the expected pinhole diameter. This indicates that the transmission losses cannot be explained by modeling the transmission as simply a reduction in effective pinhole radius. Also, this suggests that the center regions of the pinhole ($r<r_1$) fill up to a sufficient Ta atomic density such that transmission through the center region is also substantially attenuated.

Analysis and Modeling

We model the 10 μm pinhole transmission by calculating the absorption of x-rays by ablated Ta material inside the pinhole. We treat the x-ray driven ablation as an isothermal expansion and assume that that ablation does not occur until the Ta wall is heat to the boiling temperature. Pinhole transmission was calculated for 10 μm pinholes

placed at 0.45 mm and 1.0 mm away from the backlighter and is plotted in Figure 3. Backlighter efficiency, η, was assumed to be 0.07%. The calculated transmission agrees well with the data. The model-calculated pinhole size at 1.2 ns, however, is approximately 4 microns, which is smaller than that observed (see figure 8). This disagreement between measured and calculated pinhole size suggests that the ablation dynamics are not modelled well by an isothermal expansion.

Summary

We have studied the pinhole closure dynamics of 5 μm and 10 μm pinholes. We have measured the transmission of 5 μm pinholes positioned 1.0 mm away from a Ti backlighter and found the timescale for pinhole closure to be 600 ps, The transmission of 10 μm pinholes positioned both 0.45 mm and 1.0 mm away from the backlighter was also measured, and the timescales for closure were 1.3 ns and 2.2 ns, respectively. The effective diameter of the 10 μm pinhole during ablation and closure was also measured by analysis of the 1-D wire shadow resolution. This analysis showed that, within the error of the measurement, that the effective pinhole diameter did not change sufficiently in time to explain the corresponding loss in transmission. This suggests that pinhole transmission losses were in part due to reduced transmission in regions near the center of the pinhole. We also showed that a simple model of pinhole closure, which assumes a constant laser-to-x-ray backlighter transmitted conversion efficiency of 0.07%, can

produce transmission curves which agree with the data. This model simulates the ablation of solid Ta as an isothermal expansion that begins after the Ta surface reaches boiling temperature, and while there is a disagreement between model and data during the beginning of ablation, the model predicts the timescale for pinhole closure well.

---

[1] KilKenny, J.D., Phys. Fluids B, **2**, 1400 (1990).

[2] Glenndinning, S.G., et.al., Rev. Sci. Intrum. **70**, 536 (1999).

[3] Glenndinning, S.G., et.al., Phys. Rev. Lett. **80**, 1904 (1998).

[4] Yaakobi, B., Shvarts, D., Epstein, R., and Su, Q., Lasers and Part. Beams **14**, 81 (1996)

[5] Smalyuk, V.A., et.al., Phys. Rev. Lett. **81**, 5342 (1998).

[6] Landen, O.L., et.al., submitted to HTDC 2000.

[7] Soures, J.M., et.al., Phys. Plasmas, **3**, 2108 (1996).

[8] Koch, J.A., et.al., Appl. Opt., **37**, 1784-95 (1998).

This work was performed under the auspices of the U.S. Department of Energy by the University of California, Lawrence Livermore National Laboratory under Contract No. W-7405-Eng-48.

Table of Figures

Figure 7. Plot of 1-D Wire Shadows. In (A), the observed shadow image produced at t = 576ps by a 10 μm pinhole placed 0.45 mm away from the backlighter is shown with modeled wire shadow. Modeled shadow was produced assuming a 10.6 μm pinhole resolution. In (B), a wire shadow produced by a 23 μm pinhole placed 1.5 mm away is shown for comparison.

Figure 8. Plot of transmission and measured pinhole size for a 10 μm pinhole placed 0.45 mm away from the backlighter. The measured pinhole size is produced by analyzing the resolution of 25 μm wire images produced with the 10 μm pinhole. The solid curve shown is the effective diameter of the pinhole for a steep Ta density profile based on the observed transmission curve.

Figure 9. Diagram of pinhole/backlighter interaction geometry.

Figure 10. Plot of calculated x-ray intensity and Ta temperature as a function of time at the pinhole wall for the laser pulses used with a 10 μm pinhole target (0.45 mm pinhole-to-backlighter distance).

Figure 11. Diagram of pinhole/backlighter interaction geometry showing the limited backlighter area visible to the regions of the Ta pinhole wall at depths of l_1 and l_2. Note that the region at the depth l_2 is illuminated with a lower backlighter x-ray intensity than the region at depth of l_1.

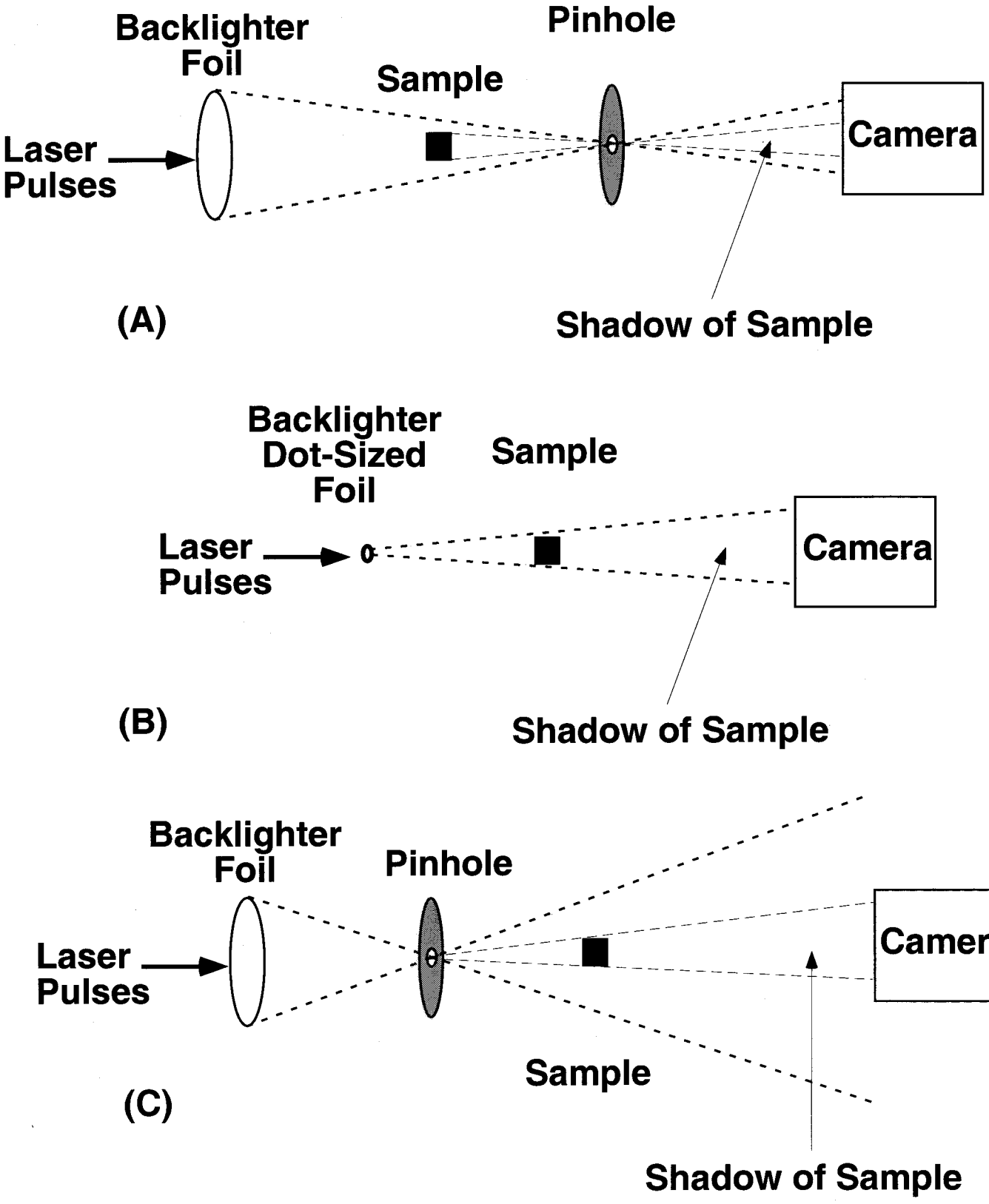
Backlighter
Foil
Pinhole
Sample
Laser
Pulses
Camera
(A)
Shadow of Sample
Backlighter
Dot-Sized
Foil
Sample
Laser
Pulses
Camera
(B)
Shadow of Sample
Backlighter
Foil
Pinhole
Laser
Pulses
Camera
Sample
(C)
Shadow of Sample

Figure 1

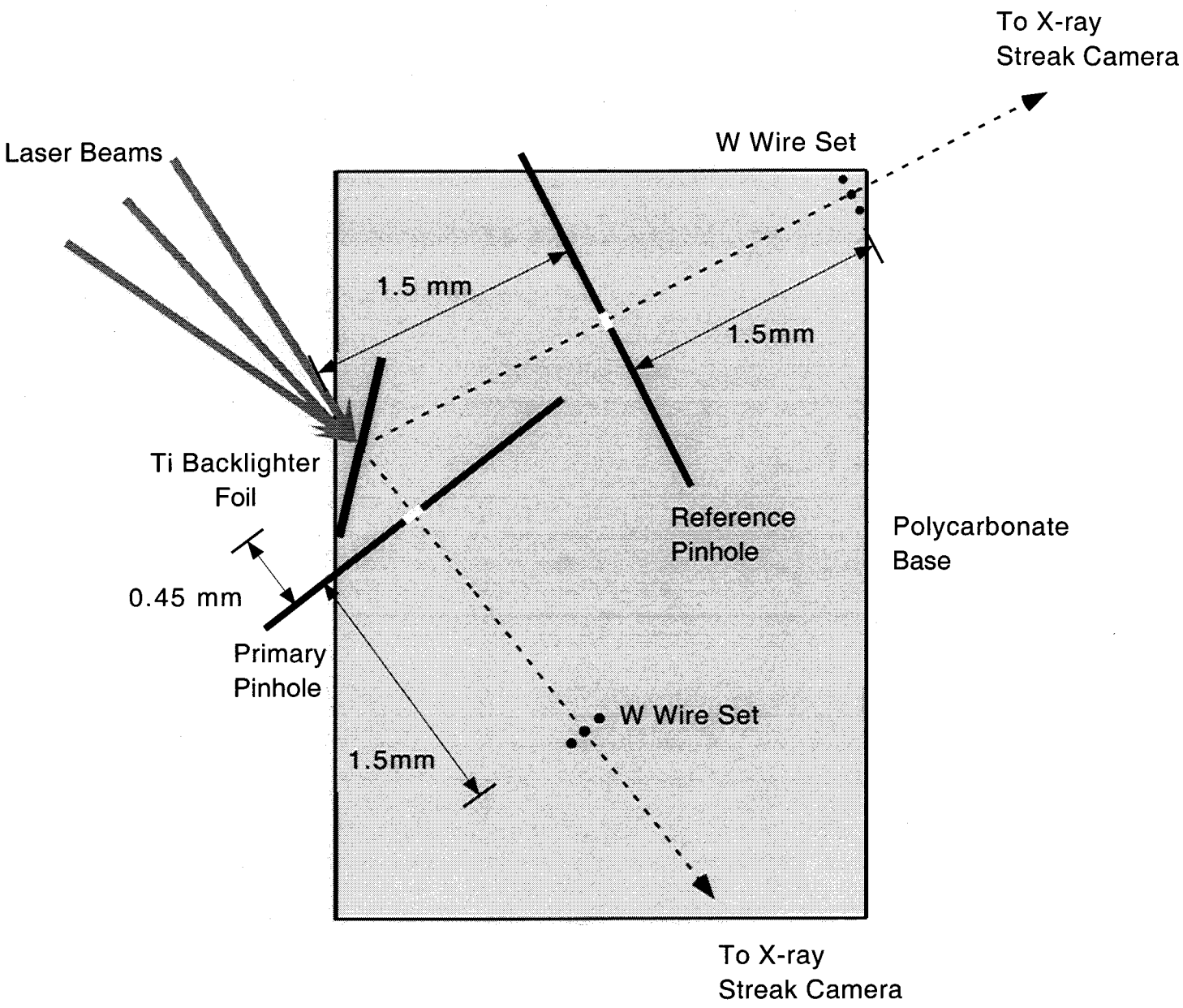
To X-ray
Streak Camera
Laser Beams
W Wire Set
1.5 mm
1.5mm
Ti Backlighter
Foil
Reference
Pinhole
Polycarbonate
Base
0.45 mm
Primary
Pinhole
W Wire Set
1.5mm
To X-ray
Streak Camera

Figure 2

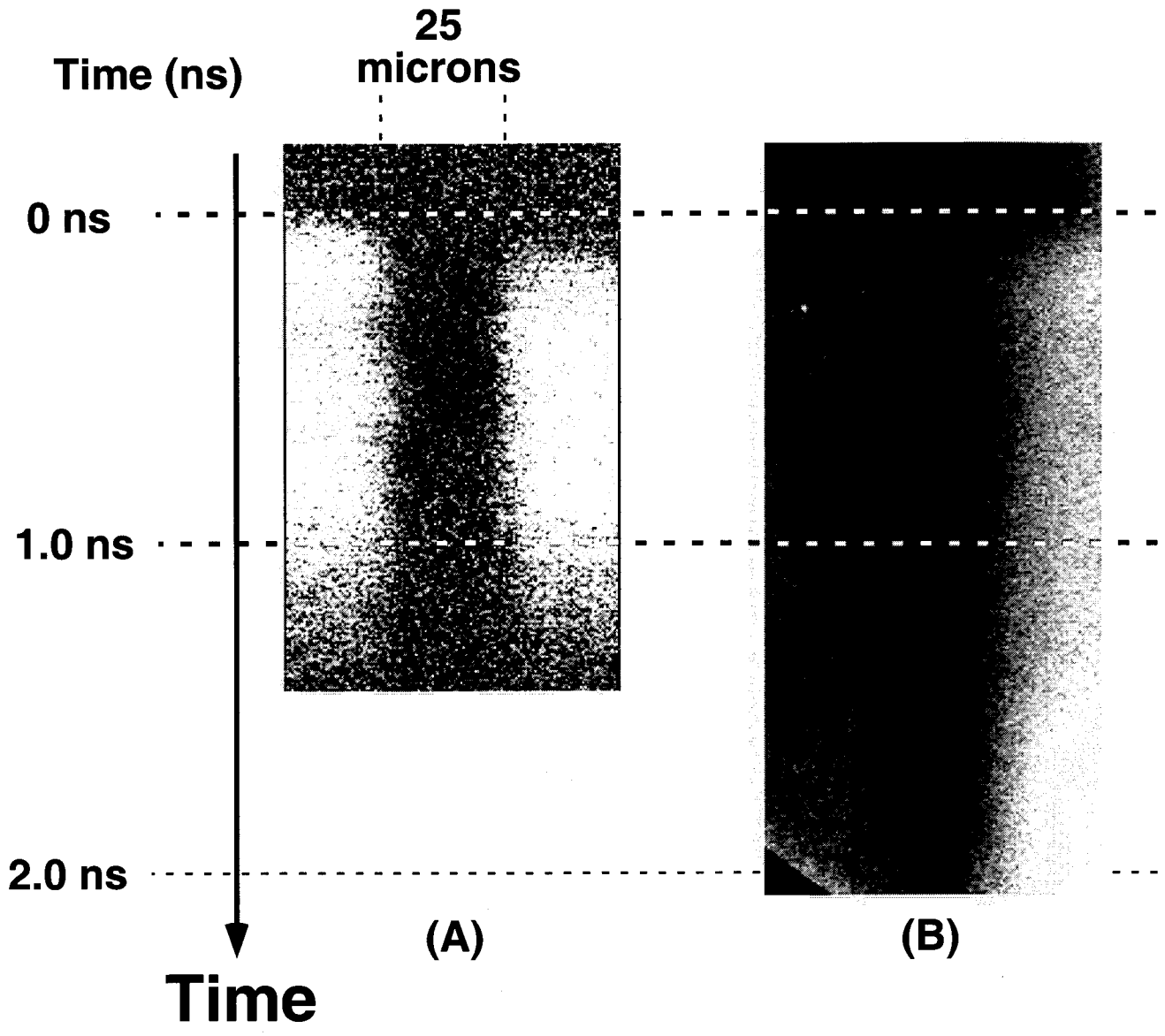

Figure 3

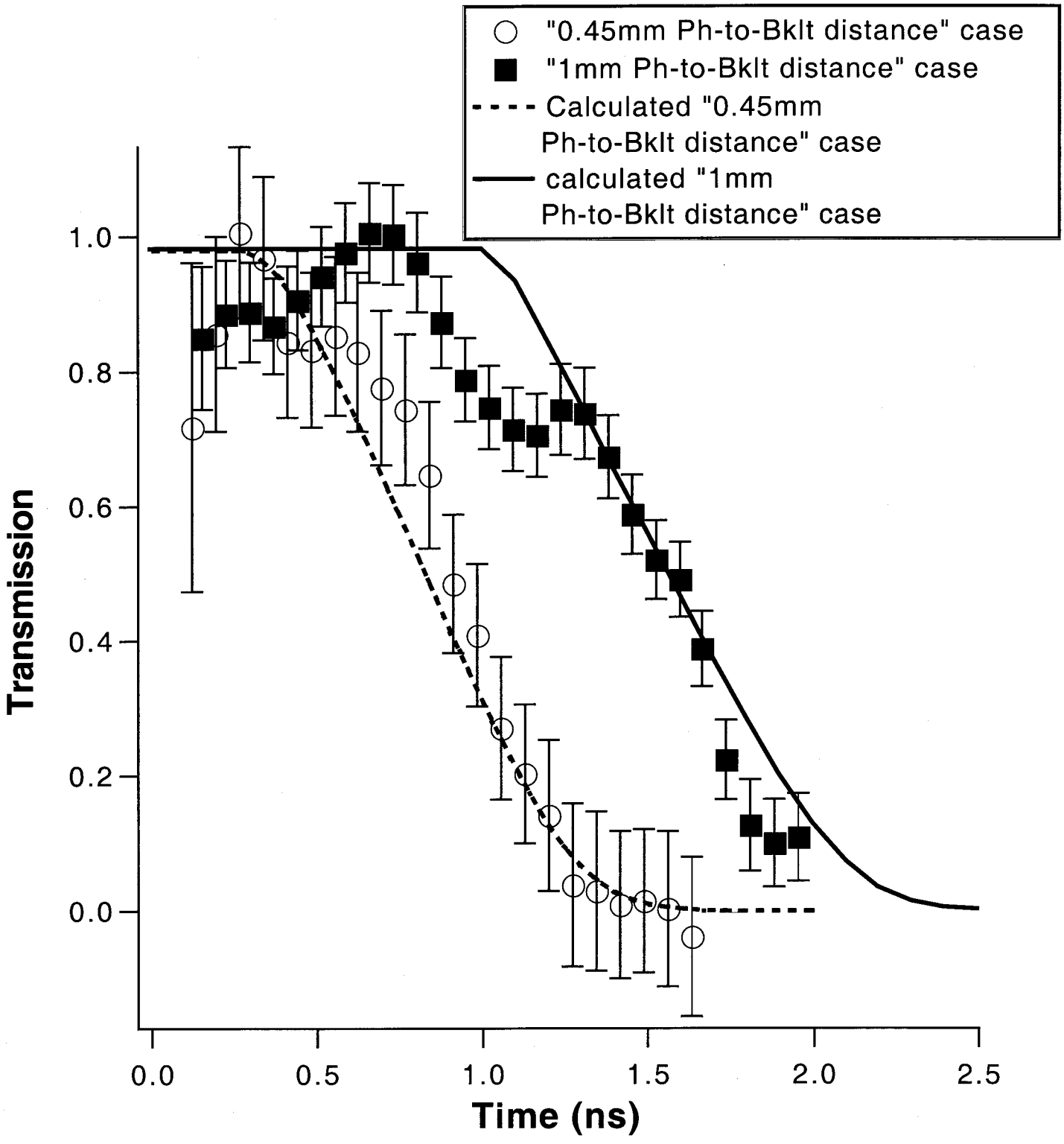
"0.45mm Ph-to-Bklt distance" case
"1mm Ph-to-Bklt distance" case
Calculated "0.45mm Ph-to-Bklt distance" case
calculated "1mm Ph-to-Bklt distance" case
Transmission
1.0
0.8
0.6
0.4
0.2
0.0
0.0
0.5
1.0
1.5
2.0
2.5
Time (ns)

Figure 4

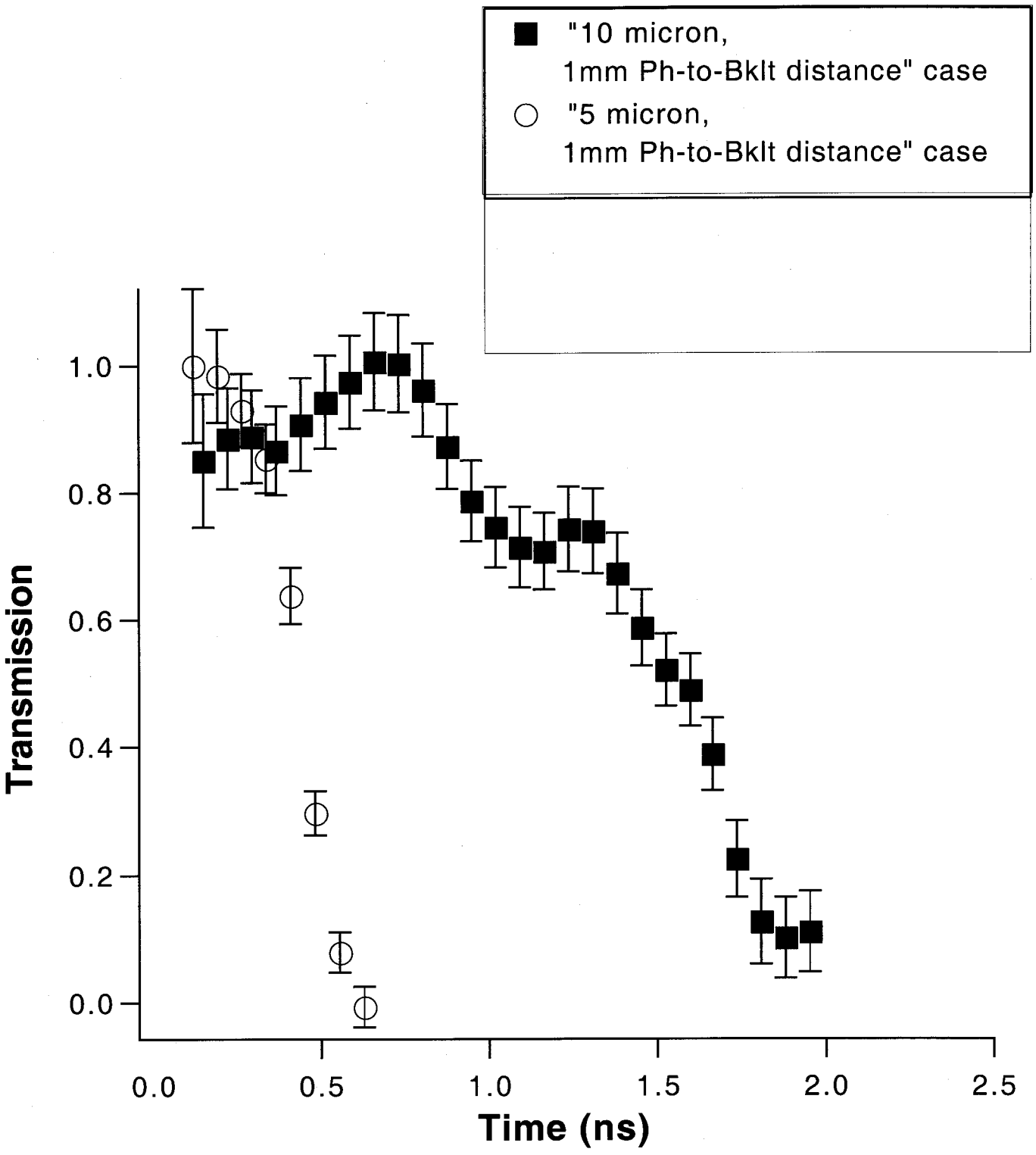
"10 micron,
1mm Ph-to-Bklt distance" case
"5 micron,
1mm Ph-to-Bklt distance" case
Transmission
1.0
0.8
0.6
0.4
0.2
0.0
0.0
0.5
1.0
1.5
2.0
2.5
Time (ns)

Figure 4

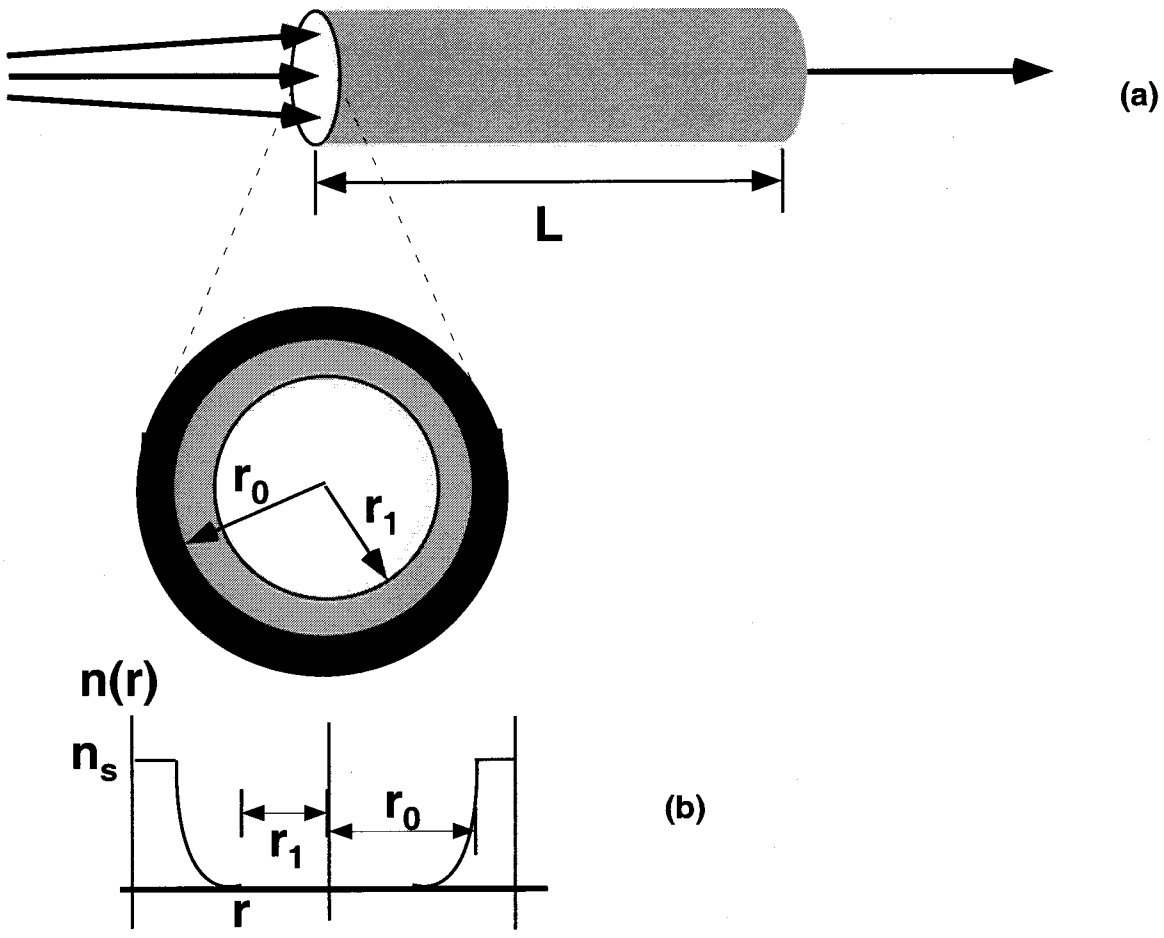

Figure 6

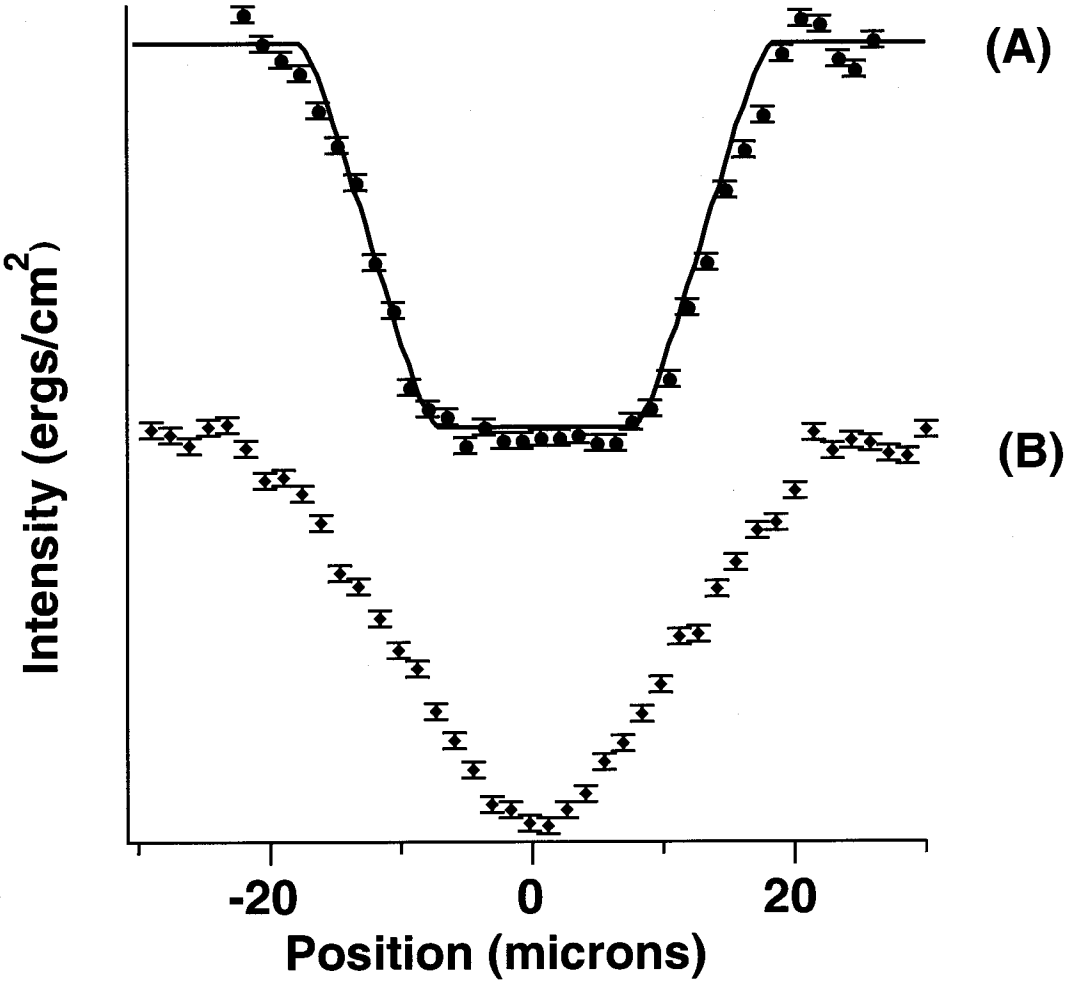

Figure 7

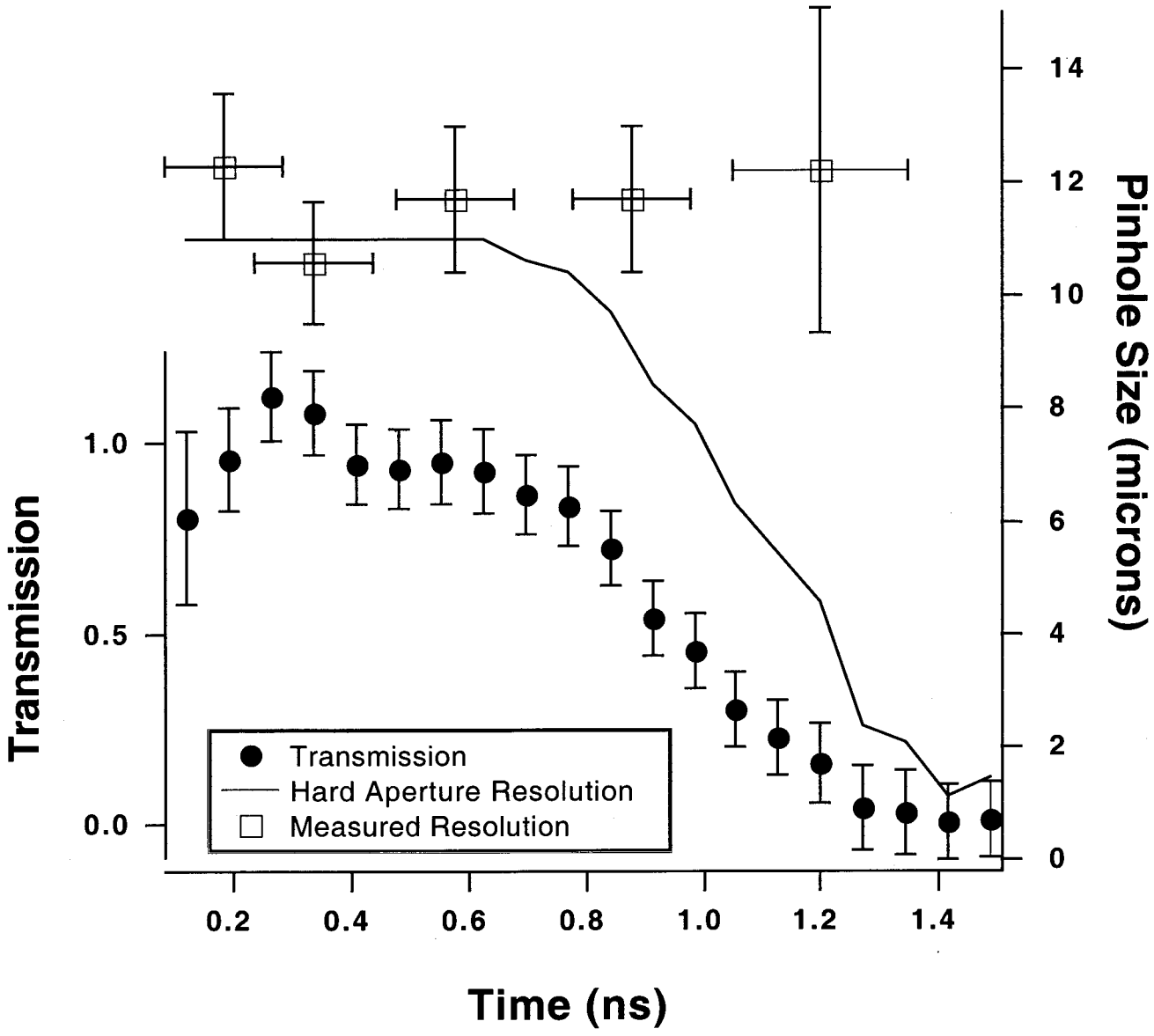
Transmission
1.0
0.5
0.0
0.2
0.4
0.6
0.8
1.0
1.2
1.4
Time (ns)
14
12
10
8
6
4
2
0
Pinhole Size (microns)
Transmission
Hard Aperture Resolution
Measured Resolution

Figure 8